DC-Link Voltage Regulation for Wind Power System by Complementary Sliding Mode Control

YANWEI HUANG[ID], ZHONGYANG ZHANG, WENCHAO HUANG, AND SHAOBIN CHEN

College of Electrical Engineering and Automation, Fuzhou University, Fuzhou 350116, China

Corresponding author: Wenchao Huang (sjtu_huanghao@fzu.edu.cn)

ABSTRACT Considering the non-rigid transmission connection between the wind turbine and the generator, their angular velocity is inconsistent. A DC-link voltage control model with uncertainties is established by a two-mass inertial model. The system uncertainties increase greatly compared with the single-mass inertial model, which aggravates a DC-link voltage accuracy. To suppress the uncertainties, the complementary sliding mode control (CSMC) is proposed to regulate the DC-link voltage since it has strong robustness. The equivalent controller for the voltage loop is obtained by the conservation principle of AC and DC side power, and the compensation controller for the uncertainties is designed by the saturation function. The CSMC system is analyzed to be asymptotic stability. The simulation and experiment results show that the CSMC system can suppress the system uncertainties, and obtain a more little steady-state error of the DC-link voltage, compared with PI control system.

INDEX TERMS Two-mass inertia model, system uncertainties, DC-link voltage regulation, complementary sliding mode control, steady-state error.

I. INTRODUCTION

In the direct-drive permanent magnet wind power system, the gear box is reduced between the wind turbine and the generator. The power generator system is easily affected by the wind speed in the direct connection mode, which leads to the ripple of DC-link voltage on the generator side. So, it is very important to adjust the DC-link voltage to suppress the wind speed variance to improve the voltage accuracy. Since the model from the wind turbine angular velocity, the DC-link voltage to generator power is nonlinear [1], this nonlinear equation can be linearized using a feedback linearization theory to obtain the state equation of the DC-link voltage and generator power. The state equation is refactored by introduced a compensation coefficient. The fluctuation amplitude of DC-link voltage can be eliminated when wind speed varies. Aiming at the problem of DC-link overvoltage caused by voltage sag of the power grid, an interval type-2 fuzzy set control method is proposed to fit the fault voltage error for power grid, to suppress the instantaneous fluctuation

The associate editor coordinating the review of this manuscript and approving it for publication was Shuping He.

of DC-link voltage [2]. To improve the output performance of the rectifier in generator side [3], the recursive wavelet neural network with an online training algorithm is used to build a tracker for the DC-link voltage. The rate of the online training algorithm is adjusted by the discrete Lyapunov function to ensure the convergence of the voltage error. This method can speed the response of the DC-link voltage response and reduce the rising time of the system response. The DC-link voltage is adjusted by the current inverter of the generator side [4]–[6]. During the case of voltage sag of power grid, the electromagnetic power of wind turbine is adjusted to convert the surplus energy into mechanical energy in the rotor of generator according to the change of DC-link voltage. This method can reduce the overvoltage of DC-link. Certainly, these methods have improved the regulation accuracy for DC-link voltage of wind turbine. However, the power generator system is assumed that the wind turbine, transmission shaft and generator are a centralized model, which simplifies the impact of wind speed fluctuation on the power generator system. This assumption neglects the non-rigid connector between the wind turbine and the generator. So, the centralized model is difficult to express the system

uncertainties caused by wind speed fluctuation on the wind turbine. Since the bending flexibility of wind turbine blade and the flexibility of transmission shaft between wind turbine and generator have an adverse impact on the transient characteristics of the wind power system [7], the control model of wind power system with three-mass, namely wind turbine blade, wind turbine and generator, is established to analyze the quantitative uncertainties caused by wind speed fluctuation. The three-mass model can more accurately describe the input speed and torque of the generator by compared with single-mass model in the same wind speed for generator [8]. A method of fractional order PID is proposed to regulate DC-link voltage to effectively improve the accuracy of voltage by weakening the system disturbance uncertainties.

The three-mass wind power system model can more accurately describe the dynamic characteristics of the system [8]–[11], especially the system uncertainties caused by wind speed fluctuation in the system. However, the shortcomings of this model are too complex to design the control method. In the conventional wind power system, there is a pitch angle control system between the wind turbine and the blades, which greatly improves the joint stiffness of the two-mass. Therefore, ignoring the flexibility between the wind turbine and the blades, the wind turbine can be simplified into a two-mass model, which consists of the wind turbine model and the generator model. This model does not affect the analysis of the system uncertainties and facilitates the design of voltage regulation system. Therefore, it is of great practical significance to establish the two-mass inertia model of wind turbine and generator. The two-mass inertia model is easy to analyze the relationship between the system uncertainties and the wind speed on the wind power system, and is explored a new control strategies to suppress the system uncertainties to reduce voltage ripple and obtain more accurate DC-link voltage.

The sliding mode control strategy has the characteristics of strong robustness and anti-interference, and it has better application performance in nonlinear systems than other control strategy. A disturbance observer-based fuzzy sliding mode control strategy is proposed for a single-phase PV grid-connected inverter [12], and the simulation results show that the proposed control strategy can work reliably under different conditions with high power factor and low THD. A practical discrete-time fractional order terminal sliding mode control strategy is proposed for high-precision tracking tasks based on a linear motor [13], and the experiments show that this method can achieve fast response and considerable robustness to uncertainties. In addition, the literatures [14], [15] also adopt the sliding mode control strategy to handle the practical application problems and achieves expected improvement effect.

Complementary sliding mode control (CSMC) method is proposed to regulate the DC-link voltage to suppress the system uncertainties in the wind power system since CSMC has the advantages of simple structure, strong robustness [16], [17]. The CSMC system for the regulation of the
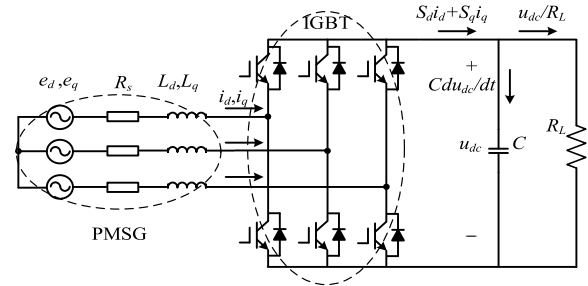

FIGURE 1. PMSG-PWM mathematical model.

DC-link voltage of the permanent magnet synchronous generator (PMSG) has a fast and accurate adjustment performance, which can effectively reduce the steady-state error of the DC-link voltage.

In a word, the contributions of this work have three points. (1) motivated by the multi-mass model for the permanent magnet wind power system[7], [8], the two-mass inertia model for the wind power system is proposed to analyze the system uncertainties with the wind speed variant by neglect of the flexibility between the wind turbine and the blades; (2) CSMC method is proposed to regulate the DC-link voltage of PMSG to suppress the system uncertainties to improve the accuracy of the DC-link voltage; (3) Through the simulations and experiments, the CSMC control method can effectively reduce the steady-state error of the DC-link voltage by compared with the PI method.

II. TWO-MASS INERTIAL MODEL WITH UNCERTAINTIES
A. PMSG-PWM RECTIFIER MODEL
The equivalent circuit diagram of PMSG and insulated gate bipolar transistor (IGBT) rectifier is shown in Fig.1. In PMSG, e_d and e_q are the induced electromotive force of the dq-axis respectively, R_s is stator resistance, L_d and L_q are the stator inductance of the dq-axis respectively, i_d and i_q are the stator current of the dq-axis respectively. In IGBT rectifier, S_d and S_q are the switching function of the rectifier of the dq-axis respectively, R_L is the load, C is the capacitance of DC-link, u_{dc} is the DC-link voltage. $S_d i_d + S_q i_q$ is the total current output of the rectifier, $C du_{dc}/dt$ is the current flowing through the capacitance of DC-link, u_{dc}/R_L is the current flowing through the load.

As shown in the Fig.1, the switch of IGBT is driven by the PWM signal, so that AC energy of the output of PMSG can be transformed to DC energy by the IGBT rectifier. Then, the PMSG-PWM mathematical model included of PMSG and IGBT rectifier can be established. In the dq-axis coordinate system, the PMSG-PWM mathematical model is:

$$\begin{cases} e_d = R_s i_d + L_d \dfrac{di_d}{dt} - \omega_g L_q i_q + S_d u_{dc} \\ e_q = R_s i_q + L_q \dfrac{di_q}{dt} + \omega_g L_d i_d + S_q u_{dc} \\ C \dfrac{du_{dc}}{dt} = \dfrac{3}{2}(S_d i_d + S_q i_q) - \dfrac{u_{dc}}{R_L} \end{cases} \tag{1}$$

where, ω_g is the electric angular velocity of generator, $\omega_g L_q i_q$ and $\omega_g L_d i_d$ are the coupling terms of PMSG dq-axis model.
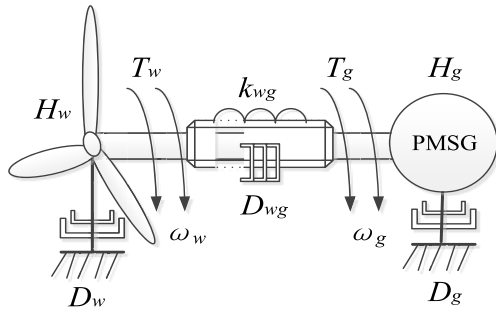
FIGURE 2. Two-mass inertial model.

These terms are regarded as the uncertainties of power generation system and directly affect the electric quantity of generator system. Moreover, the value of ω_g directly determines the sum and form of $\omega_g L_q i_q$ and $\omega_g L_d i_d$, and affects the current accuracy of the dq-axis.

B. TWO-MASS MODEL FOR WIND POWER SYSTEM

Since the transmission shaft connector between wind turbine and generator is flexible, the wind turbine and the generator are two inertial masses with consideration of the non-rigid connection in Fig.2. H_w is the equivalent inertia of the wind turbine; D_w is the damping coefficient of the wind turbine itself; T_w is the mechanical torque of the wind turbine; ω_w is the angular velocity of wind turbine; H_g is the equivalent inertia of the generator; D_g is the damping coefficient of the generator; T_g is the electromagnetic torque of the generator; k_{wg} is the stiffness coefficient of coupling; D_{wg} is the damping coefficient of coupling.

From equation (1), two-mass model of ω_g is[18],[19],

$$\begin{cases} 2H_w \dfrac{d\omega_w}{dt} = T_w - k_{wg}\theta_b - D_{wg}(\omega_w - \omega_g) - D_w\omega_w \\ 2H_g \dfrac{d\omega_g}{dt} = k_{wg}\theta_b - T_g + D_{wg}(\omega_w - \omega_g) - D_g\omega_g \\ \dfrac{d\theta_b}{dt} = \omega_0(\omega_w - \omega_g) \end{cases} \quad (2)$$

where, θ_b is the angular displacement of coupling; ω_0 is the base value coefficient of system electric angular velocity. $k_{wg}\theta_b$ is the main coupling term both the two-mass inertial model. The value of D_w and D_g are very small and can be negligible.

C. VOLTAGE DYNAMIC MODEL WITH UNCERTAINTIES

The active power output by the PMSG is conversed before and after the transformation by the rectifier [20]. That is the active power on the AC-side of the rectifier is equal to the active power on the DC-side, namely the principle of AC/DC power conservation. The voltage model can be obtained from equation (1):

$$P_{ac} = \frac{3}{2}(e_d i_d + e_q i_q) = u_{dc} i_{dc} = u_{dc} C \frac{du_{dc}}{dt} + \frac{u_{dc}^2}{R_L} = P_{dc} \quad (3)$$

where, P_{ac} is the AC power, P_{dc} is the DC power.

Equation (3) can be arranged as follows:

$$\frac{du_{dc}^2}{dt} = -\frac{2}{R_L C} u_{dc}^2 + \frac{3}{C} e_q i_q + \frac{3}{C} e_d i_d \quad (4)$$

From equation (1), the induced electromotive force e_d and e_q is affected by the generator electric angular velocity changed. Equation (1) is:

$$\begin{cases} e_d = e_{d0} + \Delta e_d = (R_s i_d + L_d \dfrac{di_d}{dt} + \omega_{g0} L_q i_q + S_d u_{dc}) \\ \qquad + \Delta\omega_g L_q i_q \\ e_q = e_{q0} + \Delta e_q = (R_s i_q + L_q \dfrac{di_q}{dt} + \omega_{g0} L_d i_d + S_q u_{dc}) \\ \qquad + \Delta\omega_g L_d i_d \end{cases}$$

$$(5)$$

where, e_{d0} is the rated induced electromotive force of the d-axis; e_{q0} is the rated induced electromotive force of the q-axis; Δe_d and Δe_q is the electromotive force deviation, $\Delta e_d = e_d - e_{d0}$, $\Delta e_q = e_q - e_{q0}$; $\Delta\omega_g$ is the angular velocity deviation of the generator, $\Delta\omega_g = \omega_g - \omega_{g0}$, ω_{g0} is the rated electric angular velocity of the generator.

Equation (4) is:

$$\frac{du_{dc}^2}{dt} = -\frac{2}{R_L C} u_{dc}^2 + \frac{3}{C} e_{q0} i_q + \frac{3}{C} e_{d0} i_d + \frac{3}{C} \Delta e_q i_q + \frac{3}{C} \Delta e_d i_d \quad (6)$$

The current loop in equation (1) is controlled by directional magnetic field, $i_d^* = 0$, so $i_d = i_d^* + \Delta i_d = \Delta i_d$. With the definition as, $v = u_{dc}^2$, $A_n = -2/(R_L C)$, $B_n = 3e_{q0}/C$, Equation (6) is,

$$\dot{v} = A_n v + B_n i_q + H \quad (7)$$

where H is the system uncertainties:

$$H = 3(\Delta\omega_g L_d \Delta i_d i_q + \Delta\omega_g L_q i_d \Delta i_q + e_{d0}\Delta i_d)/C \quad (8)$$

From equation (2) for a two-mass inertial system, ω_g is inconsistent to ω_w in the real-time caused for the impact of flexible factor of the transmission shaft. $\Delta\omega_g$ is more complex than that in single-mass inertial model. From equation (1), the induced electromotive forces, e_d and e_q are affected by $\Delta\omega_g$, resulting in the increment of system uncertainties H. It is generally assumed that $|H|$ is bounded,

$$|H| \leq D \quad (9)$$

where D is a constant.

The traditional PI control strategy is also difficult to suppress the system uncertainties $|H|$, which leads to the increment of DC-link voltage ripple. Therefore, it is necessary to explore an advanced control strategy for this system to improve the voltage transient response and suppress the DC-link voltage ripple.

III. VOLTAGE REGULATION BY CSMC

CSMC method has the advantages of simple structure and strong robustness for the uncertainties. The steady-state error by CSMC system is reduced 50% times compared with that by sliding mode control [16], [17]. CSMC method is introduced to voltage regulation in the PMSG-PWM control.

A voltage error e is defined as,

$$e = v^* - v \tag{10}$$

where, v^* is the reference input signal. A generalized sliding mode surface is defined as,

$$S_g = (\frac{d}{dt} + \lambda) \int_0^t e(\tau) \, d\tau \tag{11}$$

where, λ is the design parameter of sliding mode surface, $\lambda > 0$. The derivative of the sliding surface S_g is

$$\dot{S}_g = \dot{e} + \lambda e \tag{12}$$

From equation (10) and equation (7), equation (12) is expressed as,

$$\dot{S}_g = \dot{v}^* - (A_n v + B_n i_q + H) + \lambda e \tag{13}$$

To suppress the system uncertainties $|H|$ and reduce the system steady-state error, the supplementary sliding mode surface S_c is designed as

$$S_c = (\frac{d}{dt} - \lambda) \int_0^t e(\tau) \, d\tau \tag{14}$$

The two sliding mode surfaces have the following relationship:

$$\dot{S}_g = \lambda(S_g + S_c) + \dot{S}_c \tag{15}$$

The Lapunov function of CSMC system is defined as,

$$V(t) = \frac{1}{2}(S_g^2 + S_c^2) \tag{16}$$

The derivative of $V(t)$ with respect to time t is,

$$\dot{V}(t) = S_g \dot{S}_g + S_c \dot{S}_c \tag{17}$$

From equation (15), the equation (17) is,

$$\dot{V}(t) = (S_g + S_c)(\dot{S}_g - \lambda S_c) \tag{18}$$

From equation (13), equation (18) is,

$$\dot{V}(t) = (S_g + S_c)(\dot{v}^* - (A_n v + B_n i_q + H) + \lambda e - \lambda S_c) \tag{19}$$

The controlled quantity is assumed as $i_q = i_{eq} + \Delta i_q$,

$$i_{eq} = \frac{1}{B_n}(\dot{v}^* - A_n v + \lambda e + \lambda S_g) \tag{20}$$

$$\Delta i_q = \frac{1}{B_n}[\rho sat(\frac{S_g + S_c}{\phi})] \tag{21}$$

where, i_{eq} is the equivalent controller; Δi_q is the compensation controller for uncertainties; ρ is the gain; ϕ is the saturated boundary width; $sat(\cdot)$ is the saturation function.

From equation (20) and equation (21), equation (19) is,

$$\dot{V}(t) = -\lambda(S_g + S_c)^2 - (S_g + S_c)(\rho sat(\frac{S_g + S_c}{\phi}) + H)$$
$$\leq -\lambda(S_g + S_c)^2 + |S_g + S_c||H|$$
$$- (S_g + S_c)(\rho sat(\frac{S_g + S_c}{\phi}) + H) \tag{22}$$

when the satisfaction condition is $|S_g + S_c| > \phi$, $|H|$ is the bounded uncertainties from equation (8). As $\rho > D$, equation (22) has the result as, $-\lambda(S_g + S_c)^2 + (|H| - \rho)|S_g + S_c| < 0$.

In equation (22), $\dot{V}(t) < 0$, CSMC system is asymptotically stable in a large range. When the system enters the steady-state stage, S_g and S_c will satisfy the condition of sliding mode arrival at the same time. All phase trajectories will converge to zero along the intersection of the two sliding mode surfaces in finite time. Therefore, when CSMC system goes into the boundary layer of the saturation function, $S_g + S_c| \leq \phi$, from equation (11) and equation (14), $S_g + S_c = 2e$. For CSMC system, the steady-state error $|e| < \phi/2$ indicates that CSMC method can effectively suppress the system uncertainties.

IV. SIMULATIONS AND EXPERIMENTS

A. MATLAB SIMULATIONS

In Matlab simulations, CSMC for voltage regulation is established by two-mass inertial model for the wind power generator system. The nominal parameters of the control system are shown in Table 1. Fig.3 is the schematic diagram for voltage control system. The current inner loop adopts the directional magnetic field control strategy with PI controllers. The parameters of dq-axis current PI controller are both $k_p = 1$ and $k_i = 0.01$. CSMC strategy of $\lambda = 85$, $\rho = 4000$, $\phi = 0.1$ is applied to design the controller for the voltage outer loop. To compare the regulation performance, PI controller of $k_p = 22$, $k_i = 100$ is also used for the voltage outer loop to regulate DC-link voltage.

TABLE 1. The nominal value of system parameters.

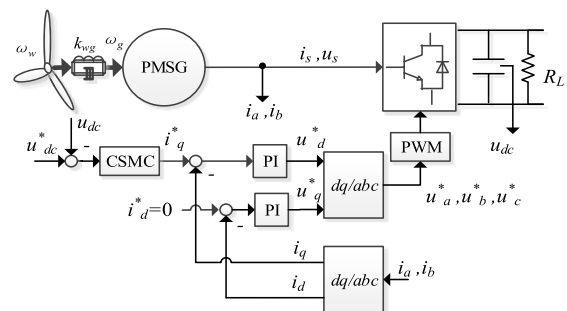| Parameters	Values	Parameters	Values
R_s	0.004054Ω	R_L	25Ω
L_d, L_q	0.3mH	C	1880uF
H_g	150kg·m^2	ω_0	5
H_w	1600kg·m^2	D_{wg}	1

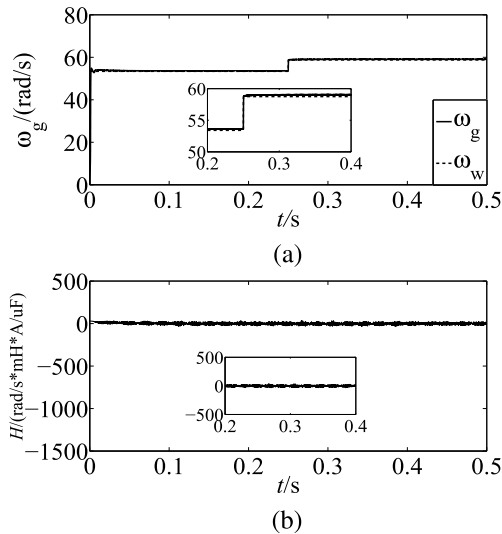**FIGURE 3.** Schematic diagram for voltage control system.

FIGURE 4. Single-mass inertial system. (a) Angular velocity ω_g. (b) Uncertainties *H*.
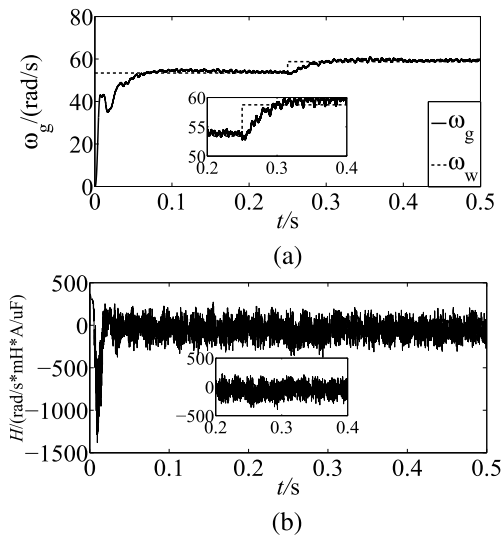

FIGURE 5. Two-mass inertial system. (a) Angular velocity ω_g. (b) Uncertainties *H*.

These control system parameters are optimal through the parameter tuning by the cross validation in experiments.

B. COMPARISONS OF SYSTEM UNCERTAINTIES

In order to analyze system uncertainties of two-mass inertial model, $k_{wg} = 6930 kg \cdot m^2/\text{rad}$ is set in simulations. When $0 < t < 0.25$s, the angular velocity of wind turbine is set $\omega_w = 17\pi \, rad/s$; when $t \geq 0.25$s, $\omega_w = 19\pi$ rad/s. Fig.4 and Fig.5 are the angular velocity ω_g and system uncertainties $|H|$ by single-mass inertial model and two-mass inertial model, respectively. Fig.4(a) shows that the angular velocity ω_g of the generator can quickly and accurately track the angular velocity ω_w. Fig.4(b) shows that the system uncertainties calculated under the single-mass model is relatively uniform, within the range of 30rad/s*mH*A/uF. Fig.5(a) shows that the generator angular velocity ω_g can't track the angular

TABLE 2. The relation between *H* and k_{wg}.

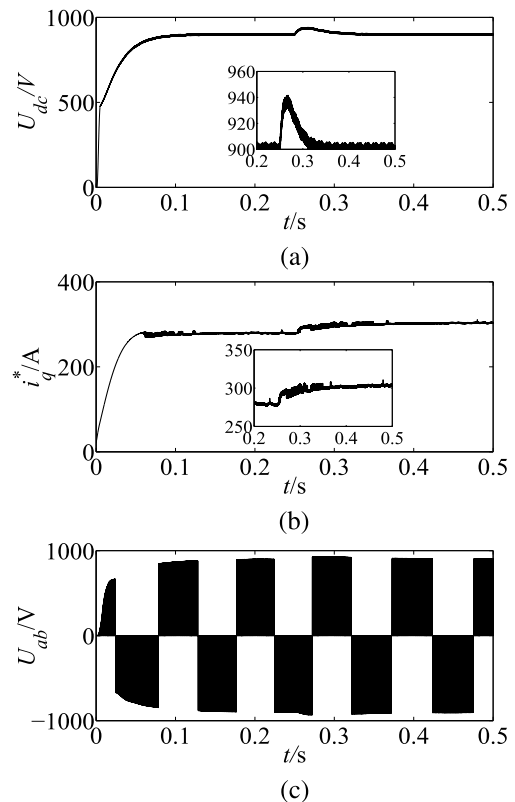| k_{wg}(kg·m^2/rad)	6930	10828	15593	21224
H(rad/s*mH*A/uF)	±300	±260	±200	±130

FIGURE 6. CSMC system. (a) U_{dc} response. (b) i_q^*. (c) U_{ab}.

velocity ω_w in real-time with the rising time t_r of about 0.04s. Moreover, the generator angular velocity ω_g fluctuates obviously, with the fluctuation amplitude of about 1.6rad/s. Fig 5(b) shows that the system uncertainties increase up to 300rad/s*mH*A/uF, about 10 times of that of single-mass model. Moreover, the system uncertainties *H* is larger up to 1200rad/s*mH*A/uF during the startup. From Fig.4 to Fig.5, the system uncertainties *H* of two-mass model are larger than that of single-mass model, since the inconsistent angular velocity from wind turbine to generator by the flexible coupling.

Table 2 shows the relationship between the system uncertainties *H* and the stiffness coefficient k_{wg} in steady state. The uncertainties *H* reduce monotonously when the stiffness coefficient k_{wg} increases.

C. VOLTAGE REGULATION BY CSMC

In simulations, $k_{wg} = 6930 kg \cdot m^2/\text{rad}$. When $0 < t < 0.25$s, the angular velocity is set $\omega_w = 17\pi + 0.575*$ random(0,1)(rad/s); when $t \geq 0.25$s, $\omega_w = 19\pi + 0.575*$ random(0,1)(rad/s). The random (0,1) is the mean to 0, the random noise variance to 1, which is used to simulate the actual wind speed fluctuations. The system performance of CSMC and PI are shown in Fig.6 and Fig.7, respectively.
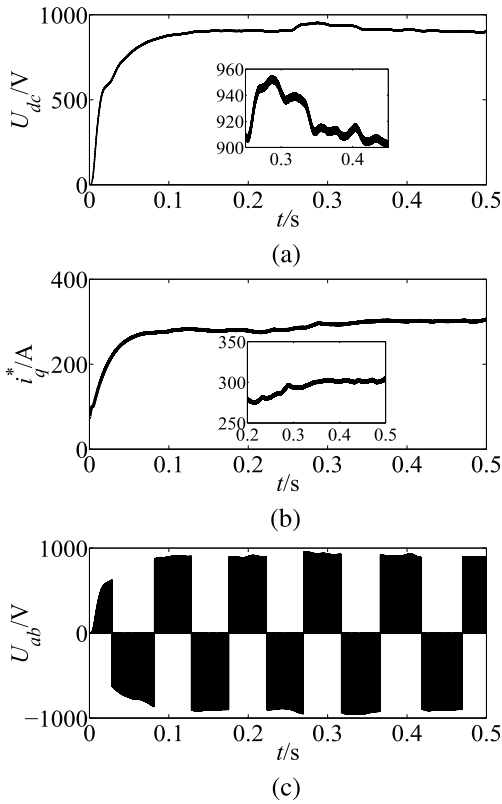
FIGURE 7. PI system. (a) U_{dc} response. (b) i_q^*. (c) U_{ab}.

**TABLE 3.** System performances with coefficient k_{wg}.

k_{wg}	CSMC		PI	
(kg·m^2/rad)	t_r(s)	e_U(V)	t_r(s)	e_U(V)
6930	0.077	±6.0	0.129	±10.6
10828	0.073	±5.6	0.115	±10.2
15593	0.067	±5.0	0.108	±9.4
21224	0.061	±4.6	0.105	±8.8

In Fig.6(a), the rising time t_r is about 0.08s, the steady state error $e_U \le \pm 6V$, where $e_U = U_{dc}^* - U_{dc}$. While the t_r is about 0.13s and $e_U \le \pm 10V$ in Fig.7(a). So the response time t_r and the steady state error e_U are smaller by CSMC than those by PI method. Fig.6(b) is the control variable i_q^* by CSMC with chattering. This chattering is produced by CSMC method in equation (21) to suppress the system uncertainties. The larger the uncertainties are, the bigger the chattering is. While the control variable i_q^* has no chattering by PI method in Fig.7(b). Fig.6(c) and Fig.7(c) are the phase voltage U_{ab} in AC sides. The phase voltage U_{ab} generated by CSMC is more orderly than that by PI method.

Table 3 shows the system performance on t_r and e_U with different stiffness coefficient k_{wg} by CSMC method and PI method. The larger the k_{wg} of the stiffness coefficient is, the shorter the response time t_r is, the smaller the steady-state error e_U of the DC-link voltage is. For example, when $k_{wg} = 21224kg \cdot m^2$/rad, the voltage response time of the CSMC system is only 80% of that when $k_{wg} = 6930kg \cdot m^2$/rad,

TABLE 4. The parameters tuning for CSMC.

| ϕ $\rho=4000$	0.04	0.06	0.08	0.1	0.12	0.14	0.16
e_U(V)	±8.8	±7.6	±6.7	±6	±7.1	±8.1	±9.2
ρ $\phi=0.1$	1000	2000	3000	4000	5000	6000	7000
e_U(V)	±12.5	±10	±7.9	±6	±7.2	±8.9	±10.3
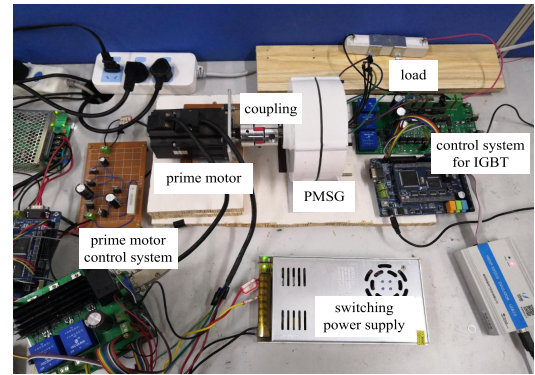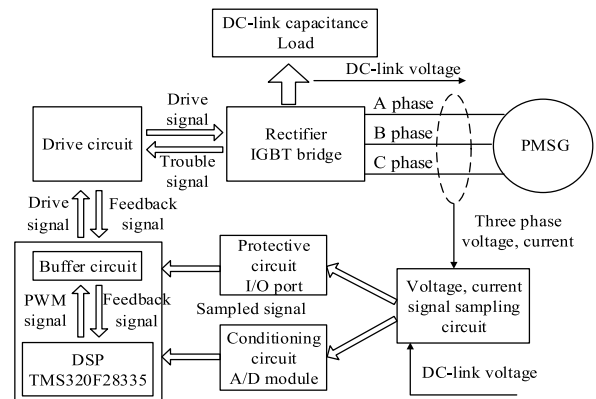
FIGURE 8. Wind power generation experimental platform. (a) Platform physical. (b) Control block diagram of PMSG rectifier.

and the steady-state error e_U is also smaller. When $k_{wg} = 21224kg \cdot m^2$/rad, the response time t_r and the steady state error e_U of the CSMC system are only 58.10% and 52.27% of those in PI control system, respectively. So, the CSMC method can accelerate the voltage response, and reduce the DC-link voltage fluctuation, since CSMC system has a strong robustness.

Table 4 shows the parameters tuning for CSMC. When $\rho = 4000$, e_U firstly decreases then increases when the parameter ϕ increases from 0.04 to 0.16 with the step of 0.02; The error e_U is minimum when $\phi = 0.1$; When $\phi = 0.1$, e_U firstly decreases then increases when the parameter ρ increases from 1000 to 7000 with the step of 1000. The error e_U is minimum when $\rho = 4000$. Therefore, it is important for CSMC to obtain an excellent system performance by parameter tuning.

TABLE 5. The parameters of motor and generator.

Motor		Generator	
Parameters	Values	Parameters	Values
Rated power P	200W	Rated power P	100W
Rated voltage U_n	48VDC	Rated voltage U_n	24V
Rated current I_n	6.5A	Rated current I_n	8A
Rated speed ω_w	100πrad/s	Rated speed ω_w	25πrad/s
Rated torque T	0.637N·m	Maximum starting resistance moment T	0.3N·m
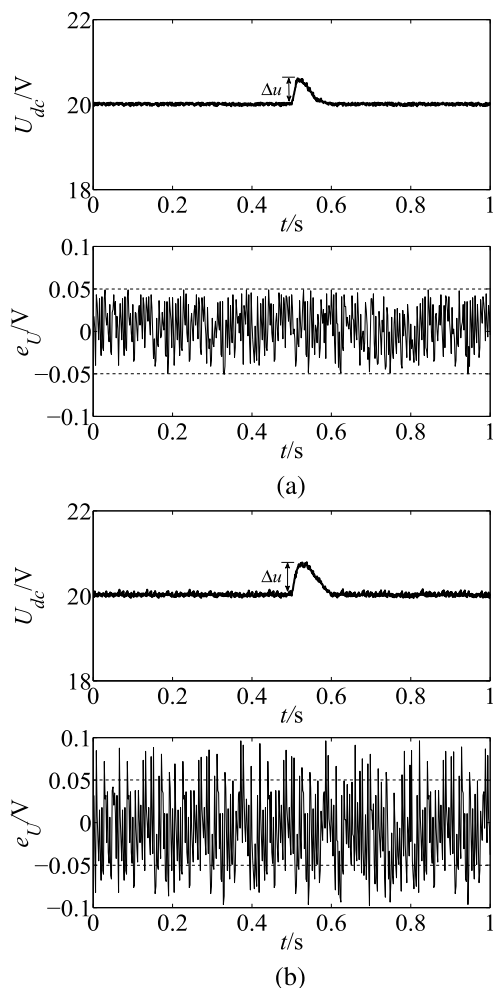
FIGURE 9. Comparisons of two control strategies. (a) CSMC regulation. (b) PI regulation.

D. EXPERIMENTAL VERIFICATION

Fig.8(a) is the experimental platform to simulate the wind power generation system, mainly composed of the prime motor, the control system for the prime motor, switching power supply, the coupling, the PMSG, the control system for IGBT, and the load. The prime motor is a servo motor to simulate wind turbine to drive the PMSG with the coupling. The type of the servo motor is SM060R20C30M0AD and PMSG is NE-100W. Fig.8(b) is the control block diagram for PMSG rectifier. Table 5 is the rated parameters of motor and PMSG. The rated parameters of switching power supply: power is 360W, voltage is 48VDC, and current is 7.5A. The load is a resistance of 100W and 8Ω. The processor for the control system for IGBT is DSP of TMS320F28335,

and the CSMC strategy is implemented by C programming language in DSP processor. Both the voltage loop and the current loop sampling frequency in the DSP control system are 20 kHz. The parameters of the CSMC controller and PI controller in the experiment are same to the optimal value in the simulations.

The prime motor velocity is that, when $0 < t < 0.5$s, $\omega_w = 20\pi$ rad/s; when 0.5s$\leq t < 1$s, $\omega_w = 25\pi$ rad/s. The DC-link voltage of PMSG is regulated to $U_{dc}^* = 20V$. These two kinds of control strategies are used to regulate the DC-link voltage U_{dc}. U_{dc} and e_U are shown in Fig.9. e_U by the PI control strategy is about ± 0.1V, but e_U by CSMC is about ± 0.05V. When the prime motor velocity ω_w increases steply from 20π to 25π rad/s at $t = 0.5$s, the voltage overshoot Δu by PI method is about 0.8V, while Δu by CSMC method is about 0.6V. So, CSMC strategy for voltage regulation can effectively suppress the uncertainties and wind variant to reduce the steady-state error e_U and the voltage overshoot Δu.

V. CONCLUSIONS

Since the wind turbine and the generator are non-rigid connected, their angular velocities are not consistent. A two-mass inertial model for wind power system is proposed to analyze the system uncertainties. The system uncertainties greatly increase by compared with the single-mass inertial model, which affects the DC-link voltage. In order to suppress the system uncertainties, CSMC method is applied to regulate the DC-link voltage because CSMC has a strong robustness to suppress the uncertainties and disturbances. Simulation and experiment results show that the transmission shaft stiffness coefficient is inversely proportional to the wind power system uncertainties, the shaft stiffness coefficient is smaller, the greater the wind power system uncertainties are. The two-mass inertial system can better simulate the actual system. At the same time, CSMC controller has a smaller response time and steady-state voltage error by compared with PI controller. Moreover, the tuning for the CSMC parameters ϕ and ρ improves the system performance. CSMC method can effectively suppress system uncertainties to reduce the steady state voltage error.

REFERENCES

[1] K.-H. Kim, Y.-C. Jeung, D.-C. Lee, and H.-G. Kim, "LVRT scheme of PMSG wind power systems based on feedback linearization," *IEEE Trans. Power Electron.*, vol. 27, no. 5, pp. 2376–2384, May 2012. doi: 10.1109/TPEL.2011. 2171999.

[2] H. M. Yassin, H. H. Hanafy, and M. M. Hallouda, "Enhancement low-voltage ride through capability of permanent magnet synchronous generator-based wind turbines using interval type-2 fuzzy control," *IET Renew. Power Gener.*, vol. 10, no. 3, pp. 339–348, Mar. 2016. doi: 10.1049/iet-rpg.2014.0453.

[3] C.-H. Lin, "Recurrent wavelet neural network control of a PMSG system based on a PMSM wind turbine emulator," *Turkish J. Elect. Eng. Comput. Sci.*, vol. 22, no. 4, pp. 795–824, Jun. 2014. doi: 10.3906/elk-1208-3.

[4] V. Yaramasu, B. Wu, S. Alepuz, and S. Kouro, "Predictive control for low-voltage ride-through enhancement of three-level-boost and NPC-converter-based PMSG wind turbine," *IEEE Trans. Ind. Electron.*, vol. 61, no. 12, pp. 6832–6843, Dec. 2014. doi: 10.1109/TIE.2014.2314060.

[5] R. Errouissi and A. Al-Durra, "A Novel PI-type Sliding Surface for PMSG-based Wind Turbine with Improved Transient Performance," *IEEE Trans. Energy Convers.*, vol. 33, no. 2, pp. 834–844, Jun. 2018. doi: 10.1109/TEC.2017.2776752.

[6] H. Geng, G. Yang, D. Xu, and B. Wu, "Unified power control for PMSG-based WECS operating under different grid conditions," *IEEE Trans. Energy Convers.*, vol. 26, no. 3, pp. 822–830, Sep. 2011. doi: 10.1109/TEC.2011.2127478.

[7] H. Li, L. Han, B. Zhao, and Z. Chen, "Effect of equivalent models of wind turbines on analysis results of transient stability for wind generator systems," *Proc. CSEE*, vol. 28, no. 17, pp. 105–111, Jun. 2008. doi: 10.13334/j.0258-8013.pcsee.2008.17.017.

[8] M. Seixas, R. Melício, and V. M. F. Mendes, "Simulation by discrete mass modeling of offshore wind turbine system with DC link," *Int. J. Mar. Energy*, vol. 14, pp. 80–100, Jun. 2016. doi: 10.1016/j.ijome.2016.02.002.

[9] L. Liu, D. Xie, H. Chu, and C. Gu, "A damping method for torsional vibrations in a DFIG wind turbine system based on small-signal analysis," *Electric Power Compon. Syst.*, vol. 45, no. 5, pp. 560–573, Mar. 2017. doi: 10.1080/15325008.2016.1274.344.

[10] H. M. Hasanien, "Shuffled frog leaping algorithm-based static synchronous compensator for transient stability improvement of a grid-connected wind farm," *IET Renew. Power Gener.*, vol. 8, no. 6, pp. 722–730, Aug. 2014. doi: 10.1049/iet-rpg.2013.0277.

[11] D. Ming, D. Wang, P. Han, J. He, and T. Hu, "Research on generalized modeling method of wind power drive-train system," *Power Syst. Technol.*, vol. 37, no. 10, pp. 2881–2887, 2013. doi: 10.13335/j.1000-3673.pst.2013.10.018.

[12] Y. Zhu and J. Fei, "Disturbance observer based fuzzy sliding mode control of PV grid connected inverter," *IEEE Access*, vol. 6, pp. 21202–21211, 2018. doi: 10.1109/ACCESS.2018.2825678.

[13] G. Sun, Z. Ma, and J. Yu, "Discrete-time fractional order terminal sliding mode tracking control for linear motor," *IEEE Trans. Ind. Electron.*, vol. 65, no. 4, pp. 3386–3394, Apr. 2017. doi: 10.1109/TIE.2017.2748045.

[14] J. Fei and C. Lu, "Adaptive fractional order sliding mode controller with neural estimator," *J. Franklin Inst.*, vol. 355, no. 5, pp. 2369–2391, Mar. 2018. doi: 10.1016/j.jfranklin.2018.01.006.

[15] H. Fukushima, K. Muro, and F. Matsuno, "Sliding-mode control for transformation to an inverted pendulum mode of a mobile robot with wheel-arms," *IEEE Trans. Ind. Electron.*, vol. 62, no. 7, pp. 4257–4266, Jul. 2015. doi: 10.1109/TIE.2014.2384475.

[16] J.-P. Su and C.-C. Wang, "Complementary sliding control of non-linear systems," *Int. J. Control*, vol. 75, no. 5, pp. 360–368, Nov. 2002. doi: 10.1080/00207170110112250.

[17] F.-J. Lin, Y.-C. Hung, and M.-T. Tsai, "Fault-tolerant control for six-phase PMSM drive system via intelligent complementary sliding-mode control using TSKFNN-AMF," *IEEE Trans. Ind. Electron.*, vol. 60, no. 12, pp. 5747–5762, Dec. 2013. doi: 10.1109/TIE.2013.2238877.

[18] D. J. Trudnowski, A. Gentile, J. M. Khan, and E. M. Petritz, "Fixed-speed wind-generator and wind-park modeling for transient stability studies," *IEEE Trans. Power Syst.*, vol. 19, no. 4, pp. 1911–1917, Nov. 2004. doi: 10.1109/TPWRS.2004.836204.

[19] M. Firouzi and G. B. Gharehpetian, "Improving fault ride-through capability of fixed-speed wind turbine by using bridge-type fault current limiter," *IEEE Trans. Energy Convers.*, vol. 28, no. 2, pp. 361–369, Jun. 2013. doi: 10.1109/TEC.2013.2248366.

[20] M. M. Zhang, Y. Li, F. Liu, L. Luo, Y. Cao, and M. Shahidehpour, "Voltage stability analysis and sliding-mode control method for rectifier in dc systems with constant power loads," *IEEE J. Emerg. Sel. Topics Power Electron.*, vol. 5, no. 4, pp. 1621–1630, Dec. 2017. doi: 10.1109/JESTPE.2017.2723482.

YANWEI HUANG received the Ph.D. degree in control theory and control engineering from Shanghai Jiao Tong University, in 2005. From 2005 to 2008, he stayed in the Research and Development Center of Enterprise to design embedded systems. He is currently a Professor with the College of Electrical Engineering and Automation, Fuzhou University.

ZHONGYANG ZHANG was born in Quanzhou, Fujian, China, in 1993. He is currently pursuing the master's degree, majoring in electrical engineering, with Fuzhou University. His main research direction is new energy generation technology.

WENCHAO HUANG received the Ph.D. degree in control theory and control engineering from Xiamen University, in 2013. He is currently a Lecturer with the College of Electrical Engineering and Automation, Fuzhou University.

SHAOBIN CHEN received the Ph.D. degree in control theory and control engineering from Zhejiang University, in 2008. He is currently an Associate Professor with the College of Electrical Engineering and Automation, Fuzhou University.

● ● ●